Available online at www.sciencedirect.com
ScienceDirect
Energy Reports 7 (2021) 579–590
www.elsevier.com/locate/egyr

Tmrees, EURACA, 28 to 30 May 2021, Athens, Greece

Sustainable fuel production from steam reforming of waste motor oil over olivine-supported Fe catalyst

Umponruch Phusuwan[a], Duangduen Atong[b], Jurarat Nisamaneenate[a], Viboon Sricharoenchaikul[a,c,*]

[a] *Department of Environmental Engineering, Faculty of Engineering, Chulalongkorn University, Bangkok 10330, Thailand*
[b] *National Metal and Materials Technology Center, Thailand Science Park, Pathumthani 12120, Thailand*
[c] *Energy Research Institute, Chulalongkorn University, Bangkok 10330, Thailand*

Received 13 July 2021; accepted 27 July 2021

Abstract

Waste Motor Oil (WMO) has great potential to be utilized as a green fuel feedstock via thermochemical process as its high carbon content is suitable as alternative source during steam reforming reactions (SR). This process not only has potential for high syngas (CO and H_2) production but also elimination of undesirable components, polyaromatic hydrocarbons (PAHs) and heavy metals in WMO. Here, evaluation of optimal conditions for WMO catalytic steam reforming in fixed-bed laboratory reactor to produce quality syngas was carried out. Influences of residence time (7–20 s), reaction temperature (700–900 °C), steam to carbon (S/C) ratio (1:2, 1:1, and 2:1), and Fe loadings (5% and 10%) on olivine support on carbon and hydrogen conversions were investigated. Results showed that the highest carbon and hydrogen conversions could be obtained after 10 s due to reactions achieving equilibrium. As for temperature, carbon and hydrogen conversions increased with temperature from mainly endothermic reactions which cause more hydrocarbon cracking. S/C volume ratio of 1:1 was preferable to obtain better carbon and hydrogen conversions due to superior heat distribution. Thus, the optimal conditions of WMO reforming were 10 s and S/C ratio of 1:1 at 800 °C which resulted in 94.68% and 79.34% carbon and hydrogen conversions, respectively, while gas product LHV was 4.44 MJ/m^3. As for Fe loading on olivine, the best performance was acquired at 800 °C, residence time of 15 s, and S/C ratio of 1:1 with 10% Fe/olivine. Carbon and hydrogen conversions increased by 7.60% to 69.91% and by 13.70% to 69.31%, respectively, when compared to non-catalytic cases. This is because of higher cracking of heavy hydrocarbons from greater Fe active sites. Application of this work may lead to decrease in environmental impact from WMO disposal and make available the green fuel for sustainable power generations or as chemical intermediates in many industries.

Peer-review under responsibility of the scientific committee of the Tmrees, EURACA, 2021.

Keywords: Waste motor oil; Steam reforming; Fe catalyst; Olivine; Syngas

* Corresponding author at: Department of Environmental Engineering, Faculty of Engineering, Chulalongkorn University, Bangkok 10330, Thailand.
E-mail address: viboon.sr@chula.ac.th (V. Sricharoenchaikul).

https://doi.org/10.1016/j.egyr.2021.07.095

Peer-review under responsibility of the scientific committee of the Tmrees, EURACA, 2021.

1. Introduction

Nowadays, various studies are more focus on alternative energy resources as relevant parties strive to introduce more feasible options to replace traditional fossil fuels (coal, oil, and natural gas). Their usages lead to negative effects on the environment from generation of CO_2, NO_x, SO_x, and other global warming and polluted gases [1,2]. There are various sources of waste that can be turned into alternative energy such as agricultural residues, animal waste, municipal waste, industrial waste, and commercial waste. WMO is particularly interesting due to its prevalent and hazardous nature and hence a significant positive environmental impact may be realized by turning it to green energy. There are 230 million liters of WMO generated in Thailand for the year 2017 [3]. This includes WMO from the automotive and industrial sectors, among others. Motor oil compounds are formed from base oils and several type of additives. Additives can serve many functions, including acting as antioxidants, corrosion and rust inhibitors, anti-foaming, anti-wear additives, extreme pressure additives, and pour point depressants [4]. After being used, these qualities and properties are lost, thus waste oils are used as solution, refining into original base oils [5], fuel reprocessing [6] and used as alternative energy. They are used in several industries such as cement, forging, wood paint, and construction. WMO poses a great threat to the environment and human health because it contains heavy metals and PAHs which are toxic and carcinogenic. Nevertheless, WMO can also be used as alternative energy source for its high hydrocarbon content, heating value, and large production which can potentially reduce the usage of fossil fuels as feedstocks.

There are several methods of utilizing waste to generate energy which depend on the properties and characteristics of particular wastes. One such method is the biological process which uses microbes to change feedstock into bioenergy (biofuels, power and heat) [7]. Another common method is the thermochemical process, which uses heat and chemical transformations to convert feedstock into energy and chemical products. There are three main modes of thermochemical process depend on the oxidizing agent availability during the reactions, namely combustion, gasification, and pyrolysis. Steam reforming is a type of gasification which occurs at high temperature to convert carbonaceous raw materials into fuel gas that may be upgraded to syngas by reaction of steam and hydrocarbon in gas phase. The advantages of steam reforming are low cost for hydrogen production, the produced gas being of higher heating value, safer and easier to control. Moreover, steam reforming can also convert some hazardous compounds such as PAHs to aliphatic compound [8] and heavy metals to ash which makes it simpler to manage as it is in solid phase [9,10].

There are several methods to improve produced gas which lead to an increase in carbon and hydrogen conversions. One of the most popular methods is the use of catalysts. This study uses Fe and olivine as the active metal and supported catalyst, respectively. Olivine is a natural mineral containing magnesium oxide, iron oxide and silica. Normally, olivine is widely used for supporting metals due to its high resistance to attrition compared to dolomite and also for its relatively low cost. The olivine's activity during steam reforming was reported as being able to remove more tar than calcined dolomite [11]. It is common to add a variety of metals into olivine to improve catalytic steam reforming. Świerczyński et al. [12] reported the olivine activities and specifically olivine activation depends on its iron oxide content. Moreover, the loading metallic on the supported material is the most attractive method to enhance activities of catalytic steam reforming. The Fe as active species catalyst was able to degrade the aromatic hydrocarbon structure by C–C and C-H bond cleavage and also enhanced water–gas shift reaction and hydrogenation [13,14]. Moreover, hydrogenation was enhanced by Fe content leading to increased hydrogen production. The Fe/olivine catalysts are interesting for steam reforming because of high H_2 yield potential of over 95% on steam reforming of toluene [15]. Tar production reduced by up to 65% in catalytic gasification of biomass with Fe/olivine and the formed carbon on surface catalyst was low and can be further oxidized easily [13].

In this study, steam reforming of WMO was performed in a lab-scale with fixed-bed. The influence of the following operating parameters was studied: reaction temperature, residence times, and steam to carbon (S/C) volume ratio. To improve quality of gas, Fe loadings of 5% and 10% on olivine was investigated. The results obtained are evaluated by observing carbon and hydrogen conversions and LHV of produced gas.

2. Materials and methods

2.1. Materials

WMO was collected from a mixed-waste motor oil tank of a local car dealer in Bangkok. The proximate and ultimate analyses of WMO are provided in Table 1. Typically, carbon and hydrogen contents in WMO are 84.19%

and 13.39%, respectively which are two times higher than most biomass [16,17]. Comparing to other liquid wastes, discarded cooking oil has lower carbon and hydrogen levels (74.70 wt% and 11.90 wt%, respectively) [18] and even lesser to 43.64 wt% carbon and 5.67 wt% hydrogen in case of palm oil mill effluent using as feedstock in gasification process for hydrogen production [19]. Heating value was also analyzed by a bomb calorimeter which reported 42.16 MJ/kg in lower heating value (LHV) and 45.05 MJ/kg in higher heating value (HHV). These values are relatively high, making WMO suitable to be used as an energy source through steam reforming to produce syngas. Furthermore, heavy metal was considered by ASTM test methods as stated in Table 2. It is denoted that Zn has the highest concentration (919 mg/kg), followed by Mo (765 mg/kg) and the other heavy metals. These heavy metals would mostly be transformed into ash by the way of steam reforming and to be handles as solid waste.

Table 1. Proximate and Ultimate Analysis of WMO.

Compositions	wt.%
Ultimate analysis	
Carbon	84.19
Hydrogen	13.39
Nitrogen	4.29
Sulfur	0.48
Proximate analysis	
Moisture content	0.10
Volatile matter	96.75
Fixed carbon	2.71
Ash	0.44
LHV (MJ/kg)	42.16

Table 2. Heavy metal analysis.

Heavy metal	Result	
Fe	5.60	mg/kg
Pb	0.28	mg/kg
Cr	2.00	mg/kg
Cu	12.00	mg/kg
Ni	0.11	mg/kg
Zn	919.00	mg/kg
Mg	N/A	
Mo	765.00	mg/kg

N/A = Not available.

2.2. Catalyst preparation

The 5% and 10% Fe/olivine catalysts were prepared by wet impregnation method of fresh olivine (Sibelco) with an iron nitrate aqueous solution (Sigma-Aldrich, $Fe(NO_3)_3{\cdot}9H_2O$). The 5% and 10% Fe/olivine required 7.23 g and 14.46 g of iron nitrate, respectively, while 20 g was used for a case of fresh olivine. Next, the excess water was removed by evaporation using a hotplate stirrer at 80 °C for 3 h. After that the impregnated catalyst was dried overnight at 105 °C in an oven, followed by calcination at 900 °C for 5 h with a heating rate of 5 °C/min.

2.3. Catalyst characterization

The porosity and surface area measurement of prepared catalyst were carried out in the TriStar II plus (Micromeritics Instrument, USA). The BET analysis used nitrogen gas as the absorbent to identify specific surface area of the samples. The pore volume and pore size were calculated by Barrett, Joyner and Halenda (BJH) method. XRD patterns were analyzed by Bruker AXS model D8 Discover (Bruker, USA) with Cu–Kα radiation at 40 kV and 40 mA at room temperature. Measurements were carried out in 5–80° (2θ) with a step time of 118.2 s and a

step size of 0.02°. The structural characterizations were analyzed by scanning electron microscope (SEM) which was performed on the JEOL JSM-IT300 (JEOL, Japan).

2.4. Experimental setup and procedures

The diagram of a lab scale fixed-bed steam reforming experimental setup is displayed in Fig. 1. The main reactor is a stainless steel tube with 0.035 m inner diameter and 0.5 m in length. For the part of catalytic steam reforming, the catalyst holder (inside diameter of 0.028 m and 0.030 m in length) was placed at the exit end of the reactor to ensure full passage of evolved gas from main reactions.

The water and WMO flowrates were set to 0.5 ml/min by syringe pump with varied S/C volume ratio. Nitrogen was used as a carrier gas which would pass through the preheater at 300 °C before flowing to the reactor at the target temperature. After the reaction, the gas product passed through gas washers and an activated carbon column. The gas then passed through the air filter before going into the Gasboard-3000P portable infrared syngas analyzer (Cubic Sensor and Instrument, PRC) which quantify permanent gas (CO, H_2, C_nH_m, CO_2, and CH_4) in real time.

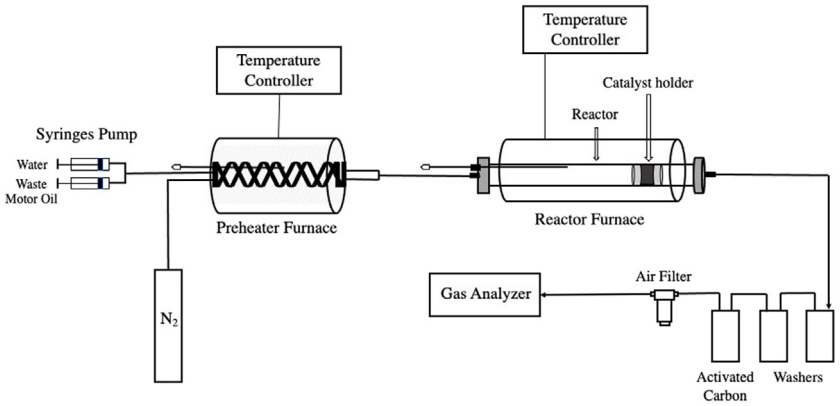

Fig. 1. Schematic of a fixed bed WMO steam reforming experiment.

3. Results and discussion

3.1. Characterization of catalysts

3.1.1. XRD analysis

The characteristics of prepared catalysts are shown in Fig. 2. The XRD patterns of the fresh olivine (Fig. 2a) exhibit the intensity of diffraction peak at $2\theta = 17.39°$, 22.88°, and 32.29°, corresponding to Mg_2SiO_4 phase which is the main component of the olivine. The diffraction peaks at $2\theta = 12.39°$ and 18.64° were $Mg_5Al(Si_3Al)O_{10}(OH)_8$. Moreover, $MgSiO_3$ phase ($2\theta = 28.12°$ and 31.12°) was also detected, comparable to report in literature [20]. When the olivine was calcined at 900 °C (Fig. 2b), the intensity of diffraction peak of Mg_2SiO_4 phase was increased at $2\theta = 22.88°$ and 32.29° while there was a decrease at $2\theta = 17.39°$. Nevertheless, the intensity of peaks of $Mg_5Al(Si_3Al)O_{10}(OH)_8$ phase disappeared whereas the increased intense peaks for $MgSiO_3$ phase were at $2\theta = 28.12°$ and 31.12°.

In the case of impregnated 5%Fe/olivine (Fig. 2c), the two diffraction peaks of Fe_2O_3 phase appeared at $2\theta = 33.17°$ and 40.86°, similar to other studies [13,14]. Due to the dehydration and oxidation of fayalite, the iron oxide phase appeared [20] while $MgSiO_3$ was detected in all catalysts. For 10%Fe/olivine, Quan et al. [21] reported that 10%Fe/olivine had a peak of Fe_2O_3 phase at $2\theta = 33.1°$ and 40.8° and those $MgSiO_3$ phase were also detected at $2\theta = 28.1°$ and 31.1°. The main crystalline phase was still Mg_2SiO_4. These were approximately the same value as 5%Fe/olivine.

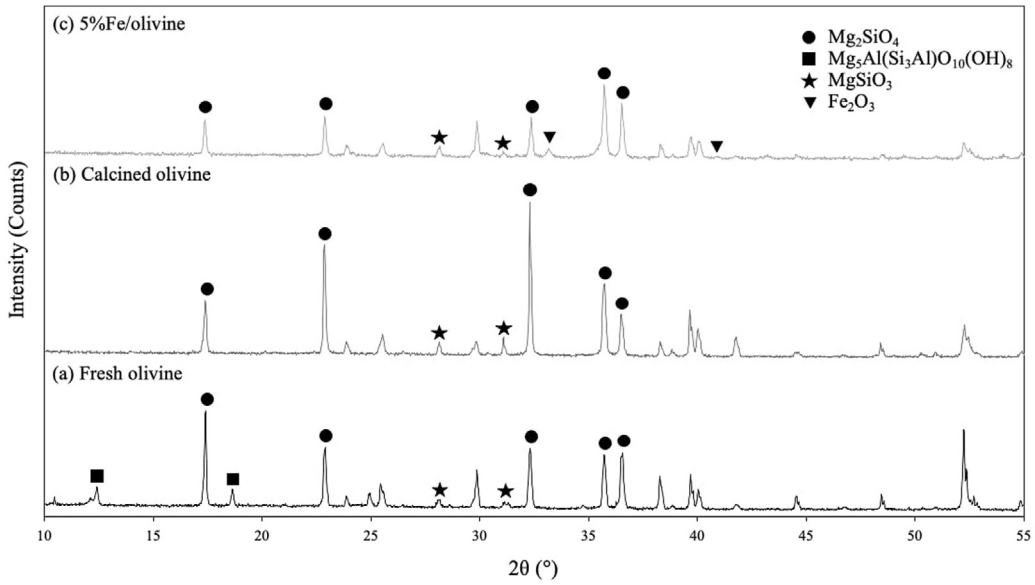

Fig. 2. X-ray diffraction (XRD) patterns of (a) fresh olivine, (b) 5%Fe/olivine, and (c) 10%Fe/olivine.

3.1.2. BET analysis

Table 3 reports the BET surface area of olivine and the different percentages of Fe content on olivine supported catalysts. Interestingly, results show that the surface area of the doped Fe catalysts increased compared to fresh olivine. Similar to Świerczyński et al. [22], the BET surface area of fresh olivine was less than 1 m^2/g. When the Fe was loaded onto olivine by 5% and 10%, the pore volume and surface area of doped Fe on olivine samples increased. Consistent with this result, Ghosal et al. [23] reported that the Fe loading content affected the physicochemical properties of olivine as well as the percentage of Fe loading which influenced their surface properties and pore structure. Greater surface area and pore volume would result in more active sites which led to the increase in hydrocarbon cracking potential.

Table 3. Physical properties of raw material and prepared catalysts.

Catalysts	S_{BET} (m^2/g)	V_t (cm^3/g)	Pore diameter (nm)
Fresh olivine	0.50	0.0010	12.37
5%Fe/olivine	1.29	0.0088	32.07
10%Fe/olivine	2.13	0.0142	31.44

3.1.3. SEM analysis

Surface morphology of fresh olivine and prepared catalysts was displayed in Fig. 3. It can be seen that fresh olivine (Fig. 3a.) has a smoother morphology than prepared catalysts. When Fe was loaded on the olivine, the surface morphology became rough due to the transformed metal–support interaction as shown in Fig. 3c and 3e. 5%Fe/olivine presents a crystalline shape from the deposit of the non-uniform size distribution and irregular morphology of iron oxide. As observed in 10%Fe/olivine, the grain size on catalyst was smaller than that of 5%Fe/olivine which led to increased surface area. Additionally, the 10%Fe/olivine seems to be of homogenous iron oxide layer on the olivine similar to the research of Virginie et al. [14]. Meng et al. [15] who proposed that the increasing Fe loading content has the stronger combined capacity of Fe and the olivine structure.

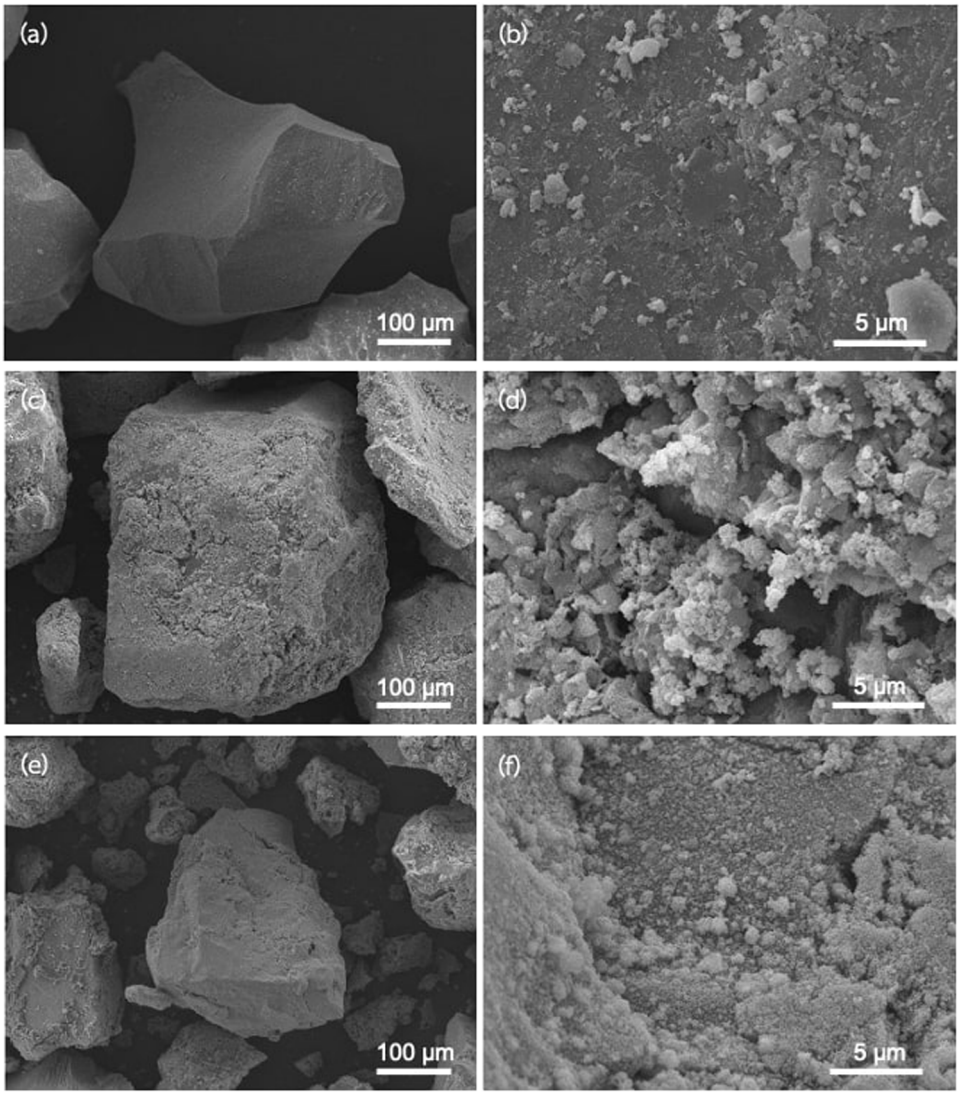

Fig. 3. SEM images of (a–b) Fresh olivine, (c–d) 5%Fe/olivine, and (e–f) 10%Fe/olivine at different magnification levels, 200X (left) and 5000X (right).

3.2. Behavior of gas composition during steam reforming

Fig. 4 shows the gas composition profile from WMO steam reforming at carrier gas residence time of 10 s. At the on set of the run, there were minute quantity of product gases being generated due to small amount of fed raw material enter the reaction zone. Gas production then increased dramatically from 9 to 12 min as ample amount of feed presented in the heated vessel. After 12 min, the gas production reached the plateau and relatively stabilized. Overall, H_2 was the major gas product followed by CO, CH_4, CO_2, and C_nH_m respectively which is comparable with Chen et al. [24] who found that from the start to 11.67 s, H_2 and CH_4 climbed dramatically but after 700 s, its reach a steady state in which H_2 and CH_4 composition in the steam–glycerol reforming were lower than in this study. The average gas compositions were about 6.07% CO, 0.94% CO_2, 8.11% H_2, 5.21% CH_4, and 0.09% C_nH_m. Furthermore, carbon and hydrogen conversions in this condition were 69.14% and 55.90%, respectively. In the part of LHV, the LHV profile was related to gas production, namely H_2, CO, and CH_4 which were obtained from the calculation, accounted as 3.57 MJ/m^3.

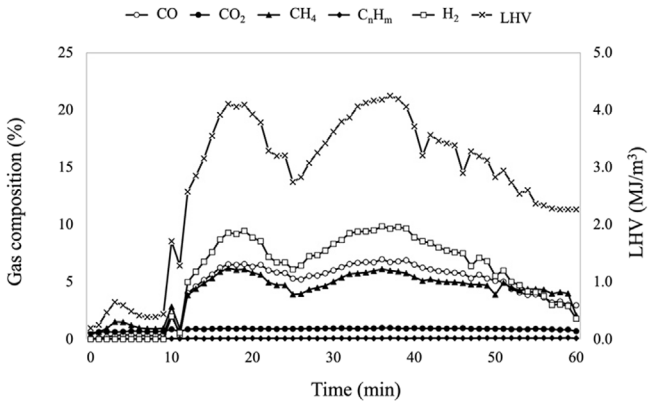

Fig. 4. Gas compositions of WMO steam reforming with residence time of 10 s at 700 °C.

3.3. Effect of residence time on carbon and hydrogen conversions

During relatively short reaction time, the steam reforming is likely be both kinetic and thermodynamic controls and hence the influence of residence time on the steam reforming of WMO was studied. Here the residence time (7, 10, 15, and 20 s) was varied by changing carrier gas flow rate at fixed S/C volume ratio of 1:1 and reaction temperature of 700 °C. The carbon and hydrogen conversions as the percentages of C or H in raw material input were plotted in Fig. 5. Significant increase in H_2 and CO conversions took place at the residence time between 7 and 10 s from 9.40% to 24.45% and 25.21% to 34.08%, respectively. On the other hand, carbon to CH_4 conversion and hydrogen to CH_4 conversion rose minimally from 26.45% to 29.79% and 27.33% to 31.45%, respectively. Meanwhile, there was minor decrease from 7.76% to 5.27% for C to CO_2 conversion. At the residence time of 15 s, CO_2, CO and CH_4 conversions declined to 3.24%, 30.36%, and 22.07%, respectively. A small increase in H_2 conversion to 26.10% was observed while H conversion as CH_4 decreased to 23.40%.

At longer residence time of 20 s, carbon conversions to CO and CH_4 also decreased gradually to 28.02% and 18.46%, respectively while there was a slight increase in CO_2 conversion to 3.71%. On the contrary, hydrogen conversions to H_2 and CH_4 decreased to 24.75% and 19.47%, respectively. Overall, changes in gas compositions were mainly due to the water–gas reaction (Eq. (1)), water–gas shift reaction (Eq. (2)), and Boudouard reaction (Eq. (3)) at higher residence time. As reported by Nanda et al. [25], the longer residence time led to an increase in H_2 and CO_2 yield due to water–gas shift reaction. Aartun et al. [26] proposed that gas production is dictated

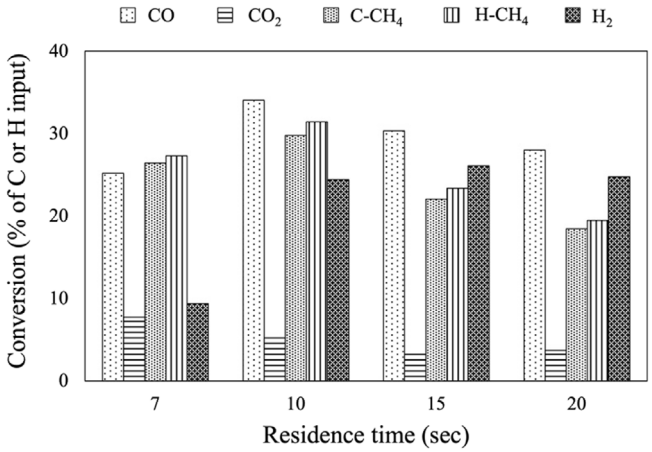

Fig. 5. Effect of residence time on carbon and hydrogen conversions with S/C volume ratio of 1:1 at 700 °C.

by equilibrium of water–gas shift reaction with the sufficient contact time. Hence the gas conversions reached the value that were close to equilibrium at the residence time of 10 s while the decrease in H_2 and CO_2 conversion with the longer residence time caused by the thermodynamic equilibrium of the reverse water–gas shift reaction.

As reported in the literature of Li et al. [27], short residence time did not promote steam activation in acetic acid steam reforming which led to retaining of more oxygen-containing functionalities. Although the longer residence time allows more chance of interaction, adequate time is required to attain the equilibrium state. Hence, excessively lower or higher residence time also affected the carbon and hydrogen conversions. These results indicated that the residence time of 10 s yielded the highest percentages of carbon and hydrogen conversions at 69.14% and 55.90%, respectively.

Water–gas reaction $C + H_2O \leftrightarrow CO + H_2$ (1)

Water–gas shift reaction $CO + H_2O \leftrightarrow CO_2 + H_2$ (2)

Boudouard reaction $C + CO_2 \leftrightarrow 2CO$ (3)

3.4. Effect of temperature on carbon and hydrogen conversions

The effect of temperature on the carbon and hydrogen conversions of steam reforming are performed at temperatures of 700, 800, and 900 °C with a S/C volume ratio of 1:1 and residence time of 10 s as shown in Fig. 6. Raising temperature to 800 °C, conversions to CO_2 and CO increased from 5.27% to 7.68% and 34.08% to 59.12% respectively, while H_2 conversion rose by over two folds from 24.45% to 49.93%. At 900 °C, the conversions of H_2 and CO seem to be more favorable as the highest values of 61.96% and 66.04%, respectively were achieved whilst CO_2 conversion sharply decreased. Meanwhile, CH_4 conversions from both carbon and hydrogen in feedstock changed slightly when the temperature rose from 700 °C to 900 °C.

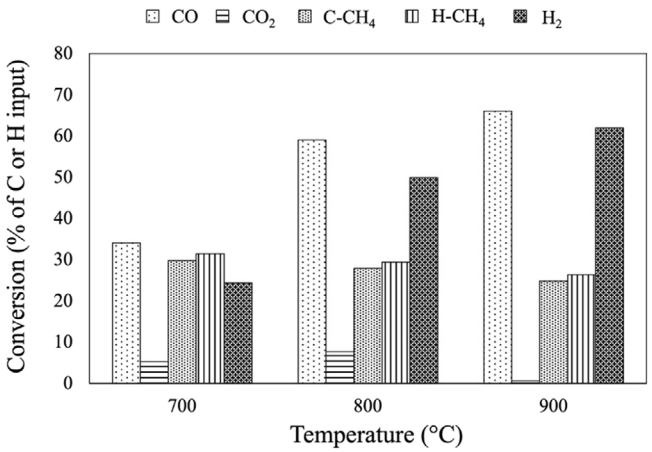

Fig. 6. Effect of temperature on carbon and hydrogen conversions with residence time of 10 s and S/C volume ratio of 1:1.

It is noticeable that increasing the temperature leads to a greater dissociation of hydrocarbon in feedstock into hydrogen and carbon monoxide due to water–gas reaction (Eq. (1)), and Boudouard reaction (Eq. (3)) as forward reactions are becoming more dominant. It is well known that reversed water–gas shift reaction (Eq. (2)) is more favorable at higher temperature and hence the level of CO would increase [28] though with the expense of H_2. CH_4 is produced by methanation reaction (Eq. (4)) while it is consumed by methane reforming reaction (Eq. (5)) and CO_2 reforming reaction (Eq. (6)) which are endothermic reactions and are favorable at higher temperatures which causes greater hydrocarbon cracking resulting in lesser CH_4. CO_2 was initially higher at 800 °C due to oxidation reaction (eqs. 7 and 8), in which oxygen is supplied by mean of water feeding though subsequently decreased by conversion to CO via Boudouard reaction (Eq. (3)). This may explain why higher temperature leads to more syngas (H_2 and CO) and lower CH_4 and CO_2.

Methanation reaction	$C + 2H_2 \leftrightarrow CH_4$	(4)
Methane reforming reaction	$CH_4 + H_2O \leftrightarrow CO + 3H_2$	(5)
CO_2 reforming reaction	$CH_4 + CO_2 \leftrightarrow 2CO + 2H_2$	(6)
Oxidation reactions	$C + O_2 \rightarrow CO_2$	(7)
	$CO + 1/2O_2 \rightarrow CO_2$	(8)

In this study the total carbon conversion to gaseous species were relatively high of 94.68% and 91.60% while LHV were 4.44 MJ/m^3 and 5.23 MJ/m^3 at 800 °C and 900 °C, respectively. As reported by Quan et al. [21], the temperature of 800 °C has the higher carbon conversion than 850 °C on the bio-oil steam reforming, accounting for 97.2% transformation. The carbon conversion to gas decreased because it changed into the solid form due to coke formation at higher temperature [29]. On the other hand, the maximum percentage of hydrogen conversion was 88.35% at 900 °C. Though the highest hydrogen conversion was at 900 °C, it was not a significant increase compared to 800 °C (79.34% hydrogen conversion) and was not worth the cost associated with increasing the temperature. Consequently, the temperature of 800 °C may be considered optimal from this perspective.

3.5. Effect of S/C volume ratio on carbon and hydrogen conversions

In this part, the influence of S/C volume ratio of 1:2, 1:1, and 2:1 on the carbon and hydrogen conversions of steam reforming are determined at 800 °C with residence time of 10 s as displayed in Fig. 7. It was observed that gas conversions were significantly affected by S/C volume ratio. The S/C volume ratio of 1:1 led to especially high levels of total carbon and hydrogen conversions at 94.68% and 79.34%, respectively. CO and H_2 conversions were the highest at 59.12% and 49.93%, respectively while CO_2 conversion was higher than those of other ratios due to water–gas reaction (Eq. (2)) and water–gas shift reaction (Eq. (3)). CH_4 conversion from carbon in feedstock varied considerably whereas that from hydrogen in feedstock changed slightly. Consequently, the S/C volume ratio of 1:1 showed the best steam reforming performance with the highest carbon and hydrogen conversions and LHV of 4.44 MJ/m^3.

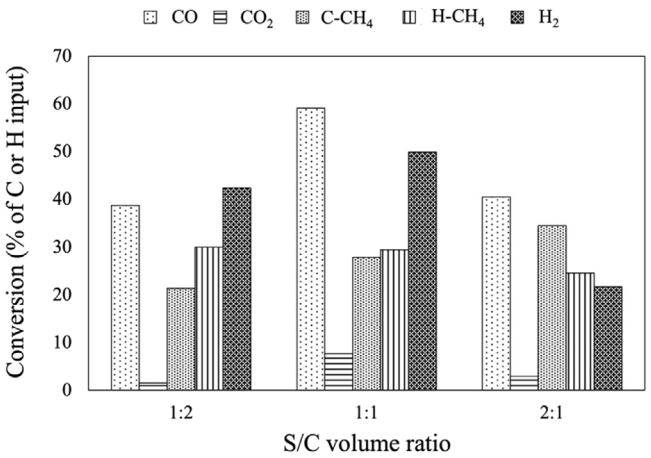

Fig. 7. Effect of S/C volume ratio on carbon and hydrogen conversions with residence time of 10 s at 800 °C.

Nanda et al. [25] studied feed concentration of waste cooking oil (WCO) and justified that the feed concentration is correlated with the volume of WCO. When the volume of WCO increased, the H_2 and CO_2 yield decreased. In addition, Aubry et al. [30] reported higher ethanol to water ratio with the decreasing of H_2 and CO_2 from 0.72 to 0.62 and from 0.10 to 0.013 (mole fractions), respectively. From steam reforming of ethanol study by Sharma et al. [31], the increase in feed concentration reduced H_2 and CO_2 selectivity from 80% to 66% and 72% to 54%, respectively and also decreased ethanol conversion to 86% from 100%. Moreover, Nabgan et al. [32] reported that the higher phenol concentration (10 to 30 wt%) in the steam reforming decreased the H_2 selectivity from 52.56% to

49.51%. These results are caused by heat transfer in which temperature is one of the important factors. The finding could be correlated to a study by Liu et al. [33] who stated that the elevated temperature increased the motion of particle molecule which has a much better opportunity to exchange heat. From this result, it can be concluded that a large amount of input (WMO and water) did not result in better heat distribution which led to lower carbon and hydrogen conversions.

3.6. Effect of catalyst addition on steam reforming process

The optimal temperature and S/C volume ratio from the previous results were at 800 °C and 1:1, respectively. In general, studying the catalytic effect uses a longer residence time so that there will be adequate time for the reaction between the substance and the catalyst to cracking and reforming reaction. Therefore, the author chose the residence time of 15 s, S/C volume ratio of 1:1 at 800 °C to study the catalytical effect on 5% and 10% Fe/olivine while the holding time in catalytic section was around 3 s. To improve the carbon and hydrogen conversions on WMO steam reforming, catalysts, namely fresh olivine, 5% Fe/olivine, and 10% Fe/olivine were used in this study. The quantity of added catalysts in each experiment was 20 g. As presented in Fig. 8, addition of catalysts resulted higher percentages of carbon and hydrogen conversions at 69.91% and 69.31% respectively, which is much higher when compared with non-catalytic cases. Among these catalysts, the lowest H_2 conversion of 37.36% was fresh olivine as catalyst and CO conversion was 40.76% though both conversions were higher when compared to non-catalysts. Moreover, CH_4 conversions from both carbon and hydrogen in WMO rose to 23.74% and 25.13%, respectively while CO_2 conversion decreased dramatically from 4.47% to 1.66%. It might be due to water–gas shift and Boudouard reactions that led to increased H_2 and CO conversions. Quan et al. [21] reported that water–gas shift reaction might be the main reason for increasing of H_2 and CO_2 components because Fe is favorable for this reaction.

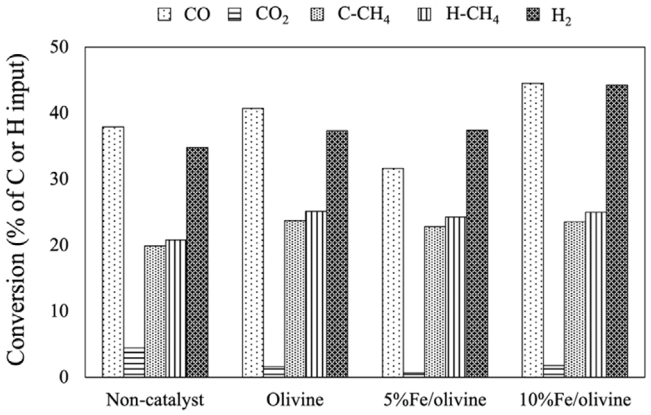

Fig. 8. Carbon and hydrogen conversions in catalytic steam reforming of WMO with residence time of 15 s and S/C volume ratio of 1:1 at 800 °C.

Additionally, the different Fe loadings on the olivine were also investigated. Increasing the Fe contents from 5% to 10% resulted in higher H_2 and CO conversions, rising from 37.44% to 44.29% and 31.65% to 44.55%, respectively. The slight increase in carbon and hydrogen conversions to CH_4 were 22.82% to 23.55% and 24.30% to 25.02%, respectively at higher Fe loadings. Although the conversion of CO_2 rose from 0.69% (5% Fe/olivine) to 1.81% (10% Fe/olivine), these values declined considerably when compared with non-catalytic trials. Consequently, 10% Fe/olivine has the highest carbon and hydrogen conversions with 6.15 MJ/m^3 of LHV.

For catalytic steam reforming, the highest carbon and hydrogen conversions was 10% Fe/olivine with 69.91% and 69.31%, respectively while 5% Fe/olivine were 55.16% and 61.74%, respectively, mainly due to the higher pore volume and surface area and also more available active sites in the 10% Fe/olivine. This led to increased carbon and hydrogen conversions and also hydrocarbon cracking. Fu et al. [28] reported the higher Fe content formed agglomerated crystals while inadequate active sites for the case of lower Fe loading led to lower efficiency. Similarly, Quan et al. [21] reported that the amount of Fe content influences catalyst activities. The carbon and hydrogen conversions rose as Fe contents increased from 5 to 20% with the highest carbon conversion of 97.20% achieved at 10% Fe/olivine of bio-oil steam reforming.

4. Conclusions

Steam reforming of WMO was studied to investigate the effects of residence time, temperature and S/C volume ratio on carbon and hydrogen conversions. The result shows that the difference in residence time and temperatures significantly affected carbon and hydrogen conversions where these conversions increased and then decreased with the former. The change in S/C volume ratio has a great effect on carbon and hydrogen conversions due to heat transfer limitation. Thereby, the lower mass flow of input (WMO and water) was favorable for thermal homogeneity (high heat transfer). The optimal conversion conditions obtained at the residence time of 10 s, temperature of 800 °C and the S/C volume ratio of 1:1. This condition showed 94.68% of carbon conversion and 79.34% of hydrogen conversion with 4.44 MJ/m^3 of LHV. For the catalytic part, 10% Fe/olivine was selected because it has the highest pore volume and surface area. The 10% Fe/olivine catalyst exhibited superior catalytic activity for steam reforming of WMO at 800 °C, residence time of 15 s, and S/C volume ratio of 1:1. The 10% Fe/olivine improved the carbon conversion to 69.91% from 62.31% and the hydrogen conversion to 69.31% from 55.61% when compared with non-catalytic trials and hence selected as optimal catalytic reforming condition. Here, LHV reached the maximum value of 6.15 MJ/m^3. Syngas (CO and H_2) obtained as products from this reaction has many applications such chemical intermediates in methanol production and precursors in Fischer–Tropsch synthesis or upgraded fuel for gas turbine and engine for heat and power purposes. Moreover, using waste to produce chemical feedstock and green energy reduces disposal at landfill thus helps mitigate greenhouse gases emission to the atmosphere.

Declaration of competing interest

The authors declare that they have no known competing financial interests or personal relationships that could have appeared to influence the work reported in this paper.

Acknowledgments

This Research is funded by Chulalongkorn University, Thailand: CU_GR_63_71_21_09. The authors would like to thank the Department of Environmental Engineering, Faculty of Engineering, Chulalongkorn University and National Metal and Materials Technology Center for their support on bench space and sample analysis.

References

[1] Chen W, Geng W. Fossil energy saving and CO_2 emissions reduction performance, and dynamic change in performance considering renewable energy input. Energy 2017;120:283–92.
[2] Wang S, Li Q, Fang C, Zhou C. The relationship between economic growth, energy consumption, and CO_2 emissions: Empirical evidence from China. Sci Total Environ 2016;542:360–71.
[3] Pollution control department. In: Danger from waste motor oil. 2017.
[4] Yash PM. Re-refining of used lubricating oil. Sci Eng Res 2015;6(3):329.
[5] Wisa Manasomboonphan SJ. Production of liquid fuels from waste lube oils used by pyrolysis process. In: 2nd international conference on biomedical engineering and technology. Singapore: 2012.
[6] Naima K, L A. Waste oils as alternative fuel for diesel engine: A review. Pet Technol Altern Fuels 2013;4(3):30–43.
[7] Liguori R, Amore A, Faraco V. Waste valorization by biotechnological conversion into added value products. Appl Microbiol Biotechnol 2013;97(14):6129–47.
[8] Zhang L, Wu W, Siqu N, Dekyi T, Zhang Y. Thermochemical catalytic-reforming conversion of municipal solid waste to hydrogen-rich synthesis gas via carbon supported catalysts. Chem Eng J 2019;361:1617–29.
[9] Wu M-H, Lin C-L, Zeng W-Y. Effect of waste incineration and gasification processes on heavy metal distribution. Fuel Process Technol 2014;125:67–72.
[10] Cui X, Shen Y, Yang Q, Kawi S, He Z, Yang X, et al. Simultaneous syngas and biochar production during heavy metal separation from Cd/Zn hyperaccumulator (Sedum alfredii) by gasification. Chem Eng J 2018;347:543–51.
[11] Rapagnà S, Jand N, Kiennemann A, Foscolo PU. Steam-gasification of biomass in a fluidised-bed of olivine particles. Biomass Bioenergy 2000;19(3):187–97.
[12] Świerczyński D, Courson C, Bedel L, Kiennemann A, Vilminot S. Oxidation reduction behavior of iron-bearing olivines $(Fe_xMg_{1-x})_2SiO_4$ used as catalysts for biomass gasification. Chem Mater 2006;18(4):897–905.
[13] Virginie M, Adánez J, Courson C, de Diego LF, García-Labiano F, Niznansky D, et al. Effect of Fe–olivine on the tar content during biomass gasification in a dual fluidized bed. Appl Catal B 2012;121–122:214–22.
[14] Virginie M, Courson C, Niznansky D, Chaoui N, Kiennemann A. Characterization and reactivity in toluene reforming of a Fe/olivine catalyst designed for gas cleanup in biomass gasification. Appl Catal B 2010;101(1):90–100.

[15] Meng J, Zhao Z, Wang X, Wu X, Zheng A, Huang Z, et al. Effects of catalyst preparation parameters and reaction operating conditions on the activity and stability of thermally fused Fe-olivine catalyst in the steam reforming of toluene. Int J Hydrogen Energy 2018;43(1):127–38.
[16] Dankwah J, Dankwah J, Boateng K, Koshy P. Utilisation of waste automotive engine oil and its blends with biomass as reductants in ironmaking. 2015.
[17] Uçar S, Özkan AR, Karagöz S. Co-pyrolysis of waste polyolefins with waste motor oil. J Anal Appl Pyrolysis 2016;119:233–41.
[18] Kim Y-D, Jung S-H, Jeong J-y, Yang W, Lee U-D. Production of producer gas from waste cooking oil in a fluidized bed reactor: Influence of low-temperature oxidation of fuel. Fuel 2015;146:125–31.
[19] Ruya PM, Lim SS, Purwadi R, Zunita M. Sustainable hydrogen production from oil palm derived wastes through autothermal operation of supercritical water gasification system. Energy 2020;208:118280.
[20] Michel R, Ammar MR, Poirier J, Simon P. Phase transformation characterization of olivine subjected to high temperature in air. Ceram Int 2013;39(5):5287–94.
[21] Quan C, Xu S, Zhou C. Steam reforming of bio-oil from coconut shell pyrolysis over Fe/olivine catalyst. Energy Convers Manage 2017;141:40–7.
[22] Świerczyński D, Libs S, Courson C, Kiennemann A. Steam reforming of tar from a biomass gasification process over Ni/olivine catalyst using toluene as a model compound. Appl Catal B 2007;74(3):211–22.
[23] Ghosal PS, Kattil KV, Yadav MK, Gupta AK. Adsorptive removal of arsenic by novel iron/olivine composite: Insights into preparation and adsorption process by response surface methodology and artificial neural network. J Environ Manag 2018;209:176–87.
[24] Chen H, Ding Y, Cong NT, Dou B, Dupont V, Ghadiri M, et al. A comparative study on hydrogen production from steam-glycerol reforming: thermodynamics and experimental. Renew Energy 2011;36(2):779–88.
[25] Nanda S, Rana R, Hunter HN, Fang Z, Dalai AK, Kozinski JA. Hydrothermal catalytic processing of waste cooking oil for hydrogen-rich syngas production. Chem Eng Sci 2019;195:935–45.
[26] Aartun I, Venvik HJ, Holmen A, Pfeifer P, Görke O, Schubert K. Temperature profiles and residence time effects during catalytic partial oxidation and oxidative steam reforming of propane in metallic microchannel reactors. Catal Today 2005;110(1):98–107.
[27] Li X, Wang Y, Fan H, Liu Q, Zhang S, Hu G, et al. Impacts of residence time on transformation of reaction intermediates and coking behaviors of acetic acid during steam reforming. J Energy Inst 2021;95:101–19.
[28] Fu P, Yi W, Li Z, Bai X, Zhang A, Li Y, et al. Investigation on hydrogen production by catalytic steam reforming of maize stalk fast pyrolysis bio-oil. Int J Hydrogen Energy 2014;39(26):13962–71.
[29] Wu C, Liu R. Carbon deposition behavior in steam reforming of bio-oil model compound for hydrogen production. Int J Hydrogen Energy 2010;35(14):7386–98.
[30] Aubry O, Met C, Khacef A, Cormier JM. On the use of a non-thermal plasma reactor for ethanol steam reforming. Chem Eng J 2005;106(3):241–7.
[31] Sharma S, Aich S, Roy B. Low temperature steam reforming of ethanol over cobalt doped bismuth vanadate [$Bi_4(V_{0\cdot90}Co_{0.10})_2O_{11-\delta}$ (BICOVOX)] catalysts for hydrogen production. J Phys Chem Solids 2021;148:109754.
[32] Nabgan B, Nabgan W, Tuan Abdullah TA, Tahir M, Gambo Y, Ibrahim M, et al. Parametric study on the steam reforming of phenol-PET solution to hydrogen production over Ni promoted on Al_2O_3-La_2O_3 catalyst. Energy Convers Manage 2017;142:127–42.
[33] Liu W, Yang F, Jiao Y, Yuan H, Zhou H. Exploring the effect of temperature on microscopic heat transfer of liquid organics by molecular dynamics simulations. J Mol Struct 2021;1237:130383.